

Observation of vortex phase singularities in Bose-Einstein condensates

S. Inouye, S. Gupta, T. Rosenband, A.P. Chikkatur,

A. Görlitz, T.L. Gustavson, A.E. Leanhardt, D.E. Pritchard, and W. Ketterle

*Department of Physics, Research Laboratory of Electronics, and MIT-Harvard Center for Ultracold Atoms,
Massachusetts Institute of Technology, Cambridge, MA 02139, USA*

(November 10, 2018)

We have observed phase singularities due to vortex excitation in Bose-Einstein condensates. Vortices were created by moving a laser beam through a condensate. They were observed as dislocations in the interference fringes formed by the stirred condensate and a second unperturbed condensate. The velocity dependence for vortex excitation and the time scale for re-establishing a uniform phase across the condensate were determined.

Quantized vortices play a key role in the dynamics of superfluid flow [1]. The nucleation of vortices determines the critical velocity for the onset of dissipation at zero temperature. In liquid helium, vortices are a source of friction between the normal fluid and the superfluid. Multiple interacting vortices can form a lattice or vortex tangle, depending on their geometry and charge.

Bose-Einstein condensates of dilute atomic gases offer a unique opportunity to study quantum hydrodynamics. The low density of the gas allows direct comparison with first principle theories. A condensate is characterized by a macroscopic wavefunction $\psi(\vec{r}) = \sqrt{\rho(\vec{r})} \exp(i\phi(\vec{r}))$, which satisfies a non-linear Schrödinger equation. The density $\rho(\vec{r})$ and the velocity field $\vec{v}_s(\vec{r})$ in the hydrodynamic equations can now be replaced by the square of the wavefunction ($\rho(\vec{r}) = |\psi(\vec{r})|^2$) and the gradient of the *phase* of the wavefunction

$$\vec{v}_s(\vec{r}) = \frac{\hbar}{m} \nabla \phi(\vec{r}), \quad (1)$$

where m is the mass of the particle.

Recently, vortices in a Bose-Einstein condensate have been realized experimentally and are currently under intensive study [2-5]. In most of this work, vortices were identified by observing the density depletion at the cores. The velocity field was inferred only indirectly, with the exception of the work on circulation in a two-component condensate [2]. The flow field of a vortex can be directly observed when the phase of the macroscopic wavefunction is measured using interferometric techniques. In this work, we created one or several vortices in one condensate and imaged its phase by interfering it with a second unperturbed condensate which served as a local oscillator.

Interferometric techniques have previously been applied either to simple geometries such as trapped or freely expanding condensates [6-8], or to read out a phase imprinted by rf- or optical fields [2,9,10]. Here we apply an interferometric technique to visualize turbulent flow.

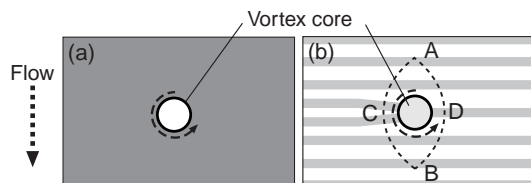


FIG. 1. Density (a) and phase (b) profile of a moving condensate with singly-charged ($n = 1$) vortex. The density profile shows the vortex core, whereas the phase pattern features a fork-like dislocation at the position of the vortex. Interference between two initially separated, freely expanding condensates produces exactly the same pattern as shown in (b), if one of the condensate contains a vortex.

The line integral of Eq. (1) around a closed path gives the quantization of circulation:

$$\int \vec{v}(\vec{r}) \cdot d\vec{r} = \frac{\hbar}{m} (\phi(\vec{r}_f) - \phi(\vec{r}_i)). \quad (2)$$

If the path is singly connected, there is no circulation. If the path is multiply connected (like around a vortex core) the circulation can take values nh/m (integer multiples of h/m), since the phase is only defined modulo 2π . As a result, the phase accumulated between two points A and B can be different depending on the path (Fig. 1). The integer quantum number n is called the charge of the vortex. When the phase gradient is integrated along a path to the left of the vortex (path ACB), the accumulated phase differs by $2n\pi$ from the path to the right (ADB).

This phase difference can be visualized with interferometric techniques. When two condensates with relative velocity v overlap, the total density shows straight interference fringes with a periodicity h/mv . If one of the condensates contains a vortex of charge n , there are n more fringes on one side of the singularity than on the other side (Fig. 1b). The change in the fringe spacing reflects the velocity field of the vortex. An observation of this fork-like dislocation in the interference fringes is a clear signature of a vortex [11].

Our setup for the interferometric observation of vortices is essentially a combination of two experiments conducted in our lab in the past [6,12]. Briefly, laser cooled sodium atoms were loaded into a double-well potential and further cooled by rf-induced evaporation below the BEC transition temperature. The double-well potential was created by adding a potential hill at the center of a cigar-shaped magnetic trap. For this, blue-detuned far off-resonant laser light (532 nm) was focused to form an elliptical $75\ \mu\text{m} \times 12\ \mu\text{m}$ (FWHM) light sheet and was aligned to the center of the magnetic trap with the long axis of the sheet perpendicular to the long axis of the condensate. The condensates produced in each well were typically $20\ \mu\text{m}$ in diameter and $100\ \mu\text{m}$ in length. The height of the optical potential was $\sim 3\ \text{kHz}$, which was slightly larger than the chemical potential of the condensate. A more intense light sheet would have increased the distance between the condensates, thus reduced the fringe spacing [6].

After two condensates each containing $\sim 1 \times 10^6$ atoms in the $F = 1, m_F = -1$ state were formed in the double-well potential, we swept a second blue-detuned laser beam through one of the condensates using an acousto-optical deflector (Fig. 2). The focal size of the sweeping laser beam ($12\ \mu\text{m} \times 12\ \mu\text{m}$, FWHM) was close to the width of the condensate. The alignment of this beam was therefore done using an expanded condensate in a weaker trap where the beam profile created a circular “hole” in the condensate density distribution.

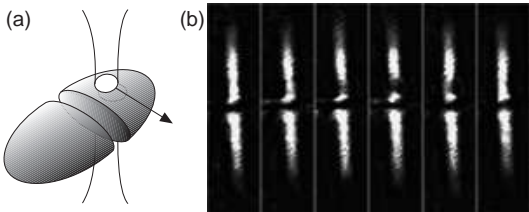


FIG. 2. Schematic (a) and phase-contrast images (b) of the condensates used for the experiment. A blue-detuned laser beam (not shown in the figure) was focused into a light sheet separating the two condensates in the magnetic trap. Another tightly focused laser beam was swept through one of the condensates (the upper one in image (b)) to excite vortices. The intensity of each laser beam was a factor of four higher than in the experiments to enhance the depleted regions in the images. The images in (b) have a field of view of $100\ \mu\text{m} \times 380\ \mu\text{m}$. For each image, the stirrer was advanced from left to right by $5\ \mu\text{m}$.

After sweeping the beam once across the “sample” condensate, the magnetic and optical fields were switched off and the two condensates expanded and overlapped during 41 ms time-of-flight. The atoms were then optically pumped into the $F = 2$ hyperfine ground state for $80\ \mu\text{s}$ and subsequently probed for $20\ \mu\text{s}$ by absorption imaging

tuned to the $F = 2$ to $F' = 3$ cycling transition.

Obtaining high contrast interference fringes ($\sim 70\%$) across the whole cloud required attention to several key factors. First, standard absorption imaging integrates along the line of sight, which was vertical in our experiment. Any bending or distortions of the interference fringes along the direction of observation would result in a loss of contrast. This was avoided by restricting the absorption of the probe light to a thin horizontal slice. The optical pumping beam was focused into a light sheet of adjustable thickness (typically $100\ \mu\text{m}$, which is about 10% of the diameter of the cloud after the time-of-flight) and a width of a few millimeters. This pumping beam propagated perpendicularly to the probe light and parallel to the long axis of the trap. Second, the number of atoms in the condensates had to be reduced to about 1×10^6 (corresponding to a chemical potential $\mu \sim 2.5\ \text{kHz}$). Higher numbers of atoms resulted in a severe loss of contrast, even if we detuned the probe beam to reduce optical density. We suspect that at high density, the two condensates do not simply interpenetrate and interfere, but interact and collide. Third, high spatial homogeneity of the probe beam was important to obtain absorption images with low technical noise. In some of our experiments, the probe beam position was actively scanned to smooth the beam profile. Fourth, the intensity of the sweeping blue-detuned beam was adjusted so that the height of the optical potential was a fraction (typically one half) of the chemical potential of the condensate. Higher intensity of the sweeping beam resulted in reduced interference fringe contrast, probably due to other forms of excitations.

Images of interfering condensates show a qualitative difference between stirred (Fig. 3(b-d)) and unperturbed states (Fig. 3(a)). Fork-like structures in the fringes were often observed for stirred condensates, whereas unperturbed condensates always showed straight fringes. The charge of the vortices can be determined from the fork-like pattern. In Fig. 3(b), vortices were excited in the condensate on top, and the higher number of fringes on the left side indicates higher relative velocity on this side, corresponding to counterclockwise flow. Fig. 3(c) shows a vortex of opposite charge. The double fork observed in Fig. 3(d) represents the phase pattern of a vortex pair. Multiply charged vortices, which are unstable against the break-up into singly charged vortices, were not observed.

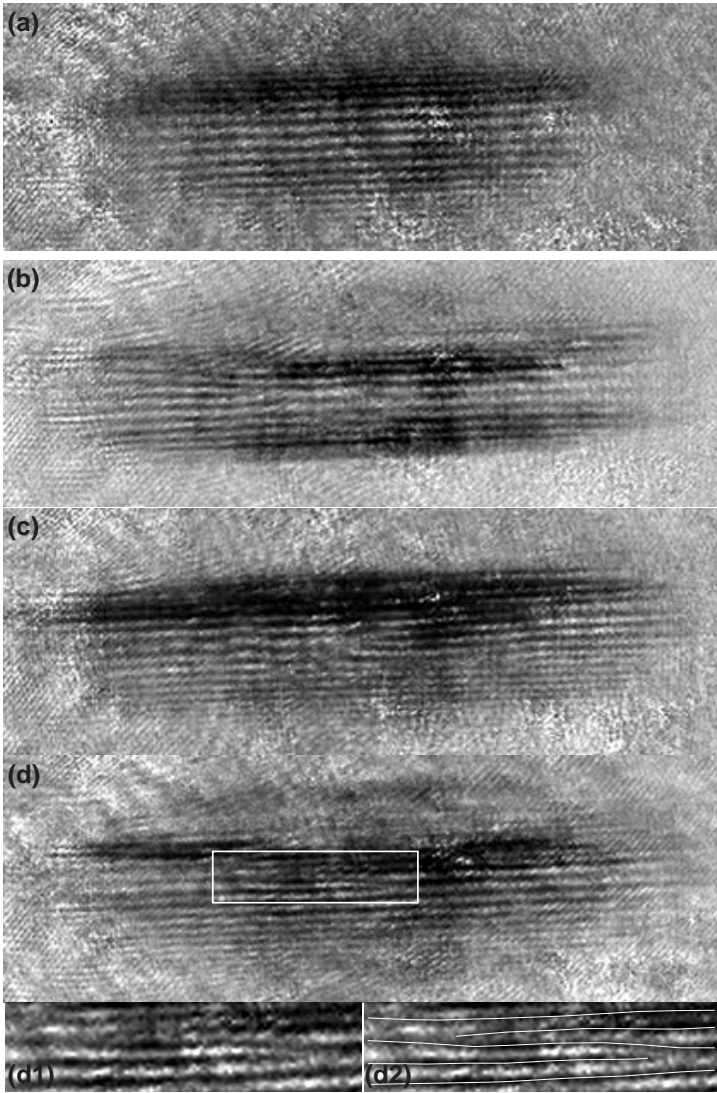


FIG. 3. Observation of the phase singularities of vortices created by sweeping a laser beam through a condensate. Without the sweep, straight fringes of $\sim 20 \mu\text{m}$ spacings were observed (a), while after the sweep, fork-like dislocations appeared (b-d). The speed of the sweep was $1.1 \mu\text{m}/\text{ms}$, corresponding to a Mach number of ~ 0.18 . The field of view of each image is $1.1 \text{ mm} \times 0.38 \text{ mm}$. Fig. (d) shows a pair of dislocations with opposite circulation characteristic of a vortex pair. At the bottom, magnified images of the fork-like structures are shown (d1) with lines to guide the eye (d2). The orientation of the condensates is the same as in Fig. 2(b).

Theoretical studies of the superfluid flow around moving objects predict dissipationless flow below a critical velocity [1]. Above this velocity, vortices of opposite circulation are created on the two sides of the moving object and give rise to a drag force [13]. A recent experiment in our group found the onset of dissipation at a critical Mach number of $v_c/c_s \sim 0.1$ [14]. Dissipation at low velocities can not only occur by vortex shedding, but also by the creation of phonons in the low density regions of

the condensate [15]. The direct observation of vortices at similar Mach numbers (Fig. 3) provides strong evidence that vortices play a major role in the onset of dissipation at the critical velocity.

By varying the speed of the laser beam sweep, we determined the velocity dependence of the vortex nucleation process. Due to the turbulent nature of the flow, every image was different even if they were taken under the same experimental conditions. Thus the images were classified by counting the number of vortices and the fractions were plotted versus the speed of the sweep (Fig. 4). The classification was done after putting images in random order to eliminate a possible “psychological bias.” The plot suggests that the nucleation of vortices requires a velocity of $\sim 0.5 \mu\text{m}/\text{ms}$, corresponding to a Mach number $v_c/c_s \sim 0.08$, consistent with our previous measurement [14]. However, a direct comparison is not possible due to different geometries—in the present experiment, the stirrer was swept along the radial direction of the condensate and almost cut the cloud completely, whereas in the previous experiment, the stirrer moved along the axial direction of an expanded condensate.

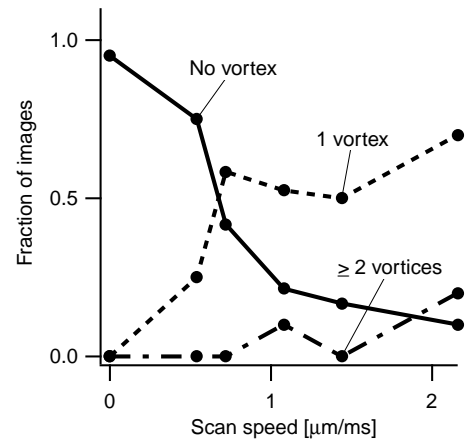


FIG. 4. Velocity dependence of vortex excitation. The fraction of images with zero (solid line), one (dashed line), and two or more vortices (dash-dotted line) are plotted versus the speed of the sweep. After the sweep, the atoms were released from the trap without delay. The total number of evaluated images was 50. Ambiguous low contrast images were excluded; therefore, the sum of the fractions is less than one.

Previous experiments have dramatically demonstrated the robustness of the long-range coherence of the condensate [6,9]. The interferometric technique used here is a sensitive way to assess whether a condensate has the assumed ground state wave function which is characterized by a uniform phase. Sweeping through the condensate excites turbulent flow. By delaying the release of the atoms from the trap by a variable amount of time, we can study the relaxation of the condensate towards its ground

state. Fig. 5 shows that the condensate completely recovers its uniform phase after 50 – 100 ms. Vortices have disappeared after ~ 30 ms. Of course, these measurements depend crucially on the specific geometry of the cloud, but they do indicate typical time scales. The sensitivity of this method was illustrated by the following observation: in a weaker trap, we saw an oscillation in time between images with straight high contrast fringes and images with low contrast fringes. This was probably due to the excitation of a sloshing motion along the weak axis of the condensate.

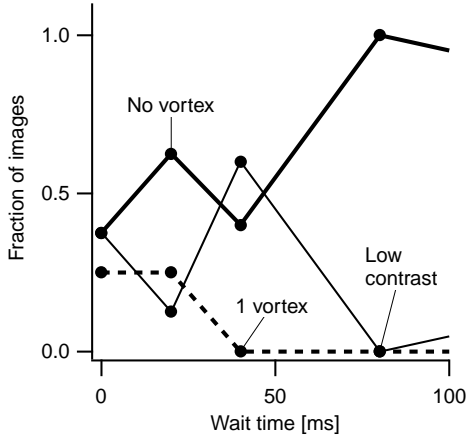


FIG. 5. Relaxation of a condensate towards uniform phase. The fraction of images with zero (thick solid line) and one (dashed line) vortex and with low contrast (thin solid line) are plotted versus the waiting time after the laser beam sweep ($v/c_s \sim 0.09$). The total number of images used for creating this plot was 33.

For interferometric detection of vortices, two different techniques have been discussed. The one employed here uses a separate condensate as a local oscillator. The other alternative is to split, shift and recombine a single condensate with vortices. In this case, the interference pattern is more complicated because all singularities and distortions appear twice. The simulations in Ref. [16] show that the self-interference technique produces more complicated fringe patterns. After completion of this work, we learned that this second technique was used in ENS, Paris to observe the phase pattern of a single vortex [17].

In conclusion, we have studied vortex excitation in Bose-Einstein condensates using an interferometric technique. This technique is suited for the study of complicated superfluid flows, e.g., when multiple vortices with opposite charges are present. We have obtained a clear visualization of vortices as topological singularities, confirmed the role of vortices in the onset of dissipation near the critical velocity, and observed the relaxation of a stirred condensate towards a state with uniform phase.

The field of Bose-Einstein condensation combines atomic and condensed matter physics. This aspect is

illustrated by this work where an atomic physics technique, matter wave interferometry, was used to probe the nucleation of vortices, a problem of many-body physics. There are many issues of vortex physics which remain unexplored, including vortices in two-dimensional condensates (condensates in lower dimensions were recently realized in our laboratory [18]), pinning of vortices by additional laser beams, and interactions between vortices.

This work was supported by NSF, the ONR, ARO, NASA, and the David and Lucile Packard Foundation. A.E.L. and A.P.C. acknowledge additional support by fellowships from NSF, and JSEP, respectively.

-
- [1] R.J. Donnelly, *Quantized Vortices in Helium II* (Cambridge University Press, Cambridge, England, 1991); P. Nozieres and D. Pines, *The Theory of Quantum Liquids* (Addison-Wesley, Redwood City, CA, 1990).
 - [2] M.R. Matthews *et al.*, Phys. Rev. Lett. **83**, 2498 (1999).
 - [3] K.W. Madison, F. Chevy, W. Wohlleben, and J. Dalibard, Phys. Rev. Lett. **84**, 806 (2000).
 - [4] B.P. Anderson *et al.*, Phys. Rev. Lett. **86**, 2926 (2001).
 - [5] J.R. Abo-Shaeer, C. Raman, J.M. Vogels, and W. Ketterle, Science, in press.
 - [6] M.R. Andrews *et al.*, Science **275**, 637 (1997).
 - [7] J.E. Simsarian *et al.*, Phys. Rev. Lett. **85**, 2040 (2000).
 - [8] I. Bloch and T. W. Hänsch and T. Esslinger, Nature **403**, 166 (2000).
 - [9] D.S. Hall, M.R. Matthews, C.E. Wieman, and E.A. Cornell, Phys. Rev. Lett. **81**, 1543 (1998).
 - [10] J. Denschlag *et al.*, Science **287**, 97 (2000).
 - [11] M.R. Andrews, Ph.D. Thesis (MIT, Cambridge, MA, 1998); E.L. Bolda and D.F. Walls, Phys. Rev. Lett. **81**, 5477 (1998); J. Tempere and J.T. Devreese, Solid State Commun. **108**, 993 (1998).
 - [12] C. Raman *et al.*, Phys. Rev. Lett., **83** 2502 (1999).
 - [13] T. Frisch, Y. Pomeau, and S. Rica, Phys. Rev. Lett. **69**, 1644 (1992); T. Winiecki, J.F. McCann, and C.S. Adams, Phys. Rev. Lett. **82**, 5186 (1999). See C. Raman, R. Onofrio, J.M. Vogels, J.R. Abo-Shaeer, and W. Ketterle, J. Low Temp. Phys. **122**, 99 (2001) for further discussions.
 - [14] R. Onofrio *et al.*, Phys. Rev. Lett. **85**, 2228 (2000).
 - [15] P.O. Fedichev and G.V. Shlyapnikov, preprint cond-mat/0004039.
 - [16] L. Dobrek *et al.*, Phys. Rev. A, **60**, R3381 (1999).
 - [17] J. Dalibard, private communication.
 - [18] A. Görlitz *et al.*, to be published.